Journal of Solar Energy Research (JSER)

Journal homepage: www.jser.ut.ac.ir

Solar-Wind Complementarity and Vortex Bladeless Turbines: A Review of VIV-Based Micro-Wind Systems for Distributed Renewable Energy

Nizar Ech-Charqaouy[a,*], Sidi Salah Ech-Charqaouy[a], Abdelkader Boulezhar[a], Amjad Ech-Charqaouy[a], Redouane Mihramane[a]

[a]*Department of physics, Faculty of Sciences of Ain Chock, Hassan II University of Casablanca, Casablanca, Morocco*

ARTICLE INFO

Article Type:

Review Article

Received:2025.10.14
Accepted in revised form:2026.02.12

Keywords:
Vortex Bladeless Turbines;
Vortex-Induced Vibrations;
Solar-Wind Hybrid Systems;
Distributed Renewable Microgrids;
CFD-FSI Modeling

A B S T R A C T

Vortex bladeless turbines (VBTs), which extract energy from vortex-induced vibrations (VIV), represent a promising class of micro-wind generators characterized by low acoustic impact, simple mechanics, and minimal wake interactions. This review consolidates advances reported between 2018 and 2025, covering Strouhal-driven shedding mechanisms, nonlinear lock-in dynamics, and recent developments in CFD-FSI simulation and reduced-order modeling. The analysis formalizes aerodynamic forcing and resonance-based power extraction, emphasizing how geometry, damping, and effective mass govern the stability, bandwidth, and durability of the oscillatory response. Progress in materials engineering - such as high-modulus composites, hybrid piezoelectric–electromagnetic converters, and tunable-stiffness architectures - strengthens fatigue resistance under harsh desert or coastal climates.

Performance evaluation is synthesized using IEC-inspired indicators and compared with conventional small HAWT and VAWT technologies. Adaptive resonance-tracking concepts, including sliding-mass systems and semi-active stiffness modules, are reviewed for maintaining synchronization under transient wind inflows. Owing to their inherently weak wake, VBTs support compact arrays and AI-assisted optimization strategies. Finally, the review discusses how the nocturnal wind profile characteristic of arid regions enables VBTs to complement daytime photovoltaic production, supporting hybrid microgrids. Key research needs include endurance testing, standardized certification, and transparent LCOE frameworks for future multi-kilowatt VBT deployment.

*Corresponding Author Email: nizarechcharqaouy@gmail.com

Cite this article: Ech-Charqaouy, N., Ech-Charqaouy, S. S., Boulezhar, A., Ech-Charqaouy, A. and Mihramane, R. Lekbir (2026). Solar-Wind Complementarity and Vortex Bladeless Turbines: A Review of VIV-Based Micro-Wind Systems for Distributed Renewable Energy. Journal of Solar Energy Research, 11(1), 2867-2890. doi: 10.22059/jser.2026.404353.1654

DOI: 10.22059/jser.2026.404353.1654

1. Introduction

The global transition toward low-carbon energy systems increasingly relies on renewable technologies capable of delivering reliable electricity under spatial, environmental, and infrastructural constraints. In high-irradiance regions such as North Africa, annual solar resources frequently exceed 2,000–2,400 kWh/m², positioning photovoltaic (PV) generation as the backbone of decentralized energy deployment [1], [2], [3]. Despite its technological maturity, PV output remains inherently intermittent due to diurnal cycles, temperature-induced efficiency losses, dust accumulation, and meteorological variability [4], [5], [6]. These fluctuations highlight the need for complementary micro-generation technologies capable of improving supply continuity and reducing reliance on large-scale storage, particularly in desert microgrids [7], [8], [9].

Wind energy represents a natural candidate for such complementarity. However, conventional horizontal-axis wind turbines (HAWTs), despite their technological maturity, continue to face deployment barriers in urban, coastal, and desert environments. Acoustic emissions, intensive maintenance requirements, avian-collision risks, and significant land occupation complicate their integration into sites where space is primarily dedicated to solar infrastructure [10], [11]. These constraints limit their synergy with PV arrays and reduce their suitability for compact hybrid renewable configurations.

Over the past decade, bladeless wind turbines (VBTs) based on vortex-induced vibrations (VIV) have emerged as a promising alternative for distributed and hybrid solar-wind systems [12], [13], [14]. Instead of harvesting rotational kinetic energy, VBTs convert oscillatory motion generated by periodic vortex shedding around a slender mast. When the vortex-shedding frequency approaches the structure's natural frequency, a lock-in regime is established, enabling efficient energy extraction at low to moderate wind speeds, conditions typically observed during evening and nighttime periods in arid climates, when PV output declines to zero [15], [16], [17].

Energy conversion in VBTs is typically achieved using piezoelectric transducers or linear electromagnetic generators incorporating oscillating magnets and stationary coils [18], [19], [20]. The absence of rotating components, bearings, and gearboxes significantly reduces acoustic emissions and mechanical wear while improving environmental compatibility and lowering maintenance requirements [21], [22], [23]. These characteristics make VBTs particularly well suited for desert environments, where sand abrasion, strong thermal cycling, and spatial limitations often hinder conventional wind technologies.

Since the commercialization of the first prototypes by Vortex Bladeless S.L. in 2018 - with nominal powers ranging from several tens of watts to nearly 4 kW - substantial progress has been achieved in understanding VIV-driven fluid-structure interactions. Recent research has addressed nonlinear stiffness behavior, aerodynamic damping mechanisms, multi-mode vibration dynamics, and enhanced electromechanical coupling strategies [24], [25], [26]. Additional innovations - including tunable resonance mechanisms, guided magnetic oscillators, multistable architectures, and morphology-optimized designs - have expanded operational wind-speed ranges and improved robustness under turbulent and gusty flow conditions [27], [28], [29].

Although VBTs generally exhibit lower specific power density than HAWTs, they provide distinct advantages in structural simplicity, lightweight construction, reduced manufacturing cost, and ease of deployment. These characteristics strengthen their relevance for hybrid PV-wind microgrids, building-integrated renewable systems, and land-constrained energy applications [30], [31], [32]. Their slender vertical geometry enables installation between PV module rows without inducing shading, thereby facilitating co-located electricity generation in high-irradiance desert regions such as Morocco and the western Sahara [33], [34].

Despite this strong potential, several scientific and technological challenges remain. Unlike small HAWTs governed by the IEC 61400-2 standard, VBTs currently lack dedicated certification procedures [20]. Existing modeling approaches vary significantly across computational fluid dynamics (CFD), fluid-structure interaction (FSI), and wake-oscillator formulations [34], [35], [36]. Long-term durability datasets remain limited [31], and validated scaling laws enabling transition from small-scale prototypes to higher-power systems are still under development [37]. Furthermore, meaningful comparisons of levelized cost of energy (LCOE) across PV, HAWTs, and VBTs remain difficult due to heterogeneous methodologies and the absence of standardized testing protocols [38], [14].

Within this context, the present review provides a comprehensive and structured synthesis of research on VIV-based micro-wind harvesters from 2018 to 2025. It examines the underlying physics, modeling approaches, prototype taxonomies, and design strategies of modern VBTs; evaluates their

integration potential within hybrid solar-wind microgrids; and highlights their suitability for high-irradiance desert regions. The review further proposes a roadmap for experimental validation, standardization, and long-term deployment, with the objective of bridging the gap between laboratory advances and real-world renewable-energy implementation.

By combining the perspectives of solar-resource complementarity and VIV-driven wind harvesting, VBTs emerge as promising enablers of modular, low-impact, and climate-resilient renewable-energy systems across North Africa and other regions characterized by high solar irradiance and moderate evening wind regimes [39], [40], [41].

2. Solar-Wind Complementarity Analysis

The integration of Vortex Bladeless Turbines (VBTs) into solar-dominated microgrids is primarily motivated by the strong temporal, seasonal, and geographical complementarity between solar irradiance and near-surface wind fields. Numerous studies confirm that hybrid solar-wind systems achieve higher reliability, smoother net-load profiles, and reduced dependence on large-scale storage compared with single-source configurations [7], [8], [9], [42], [43]. In North Africa - with the Moroccan Sahara as a prominent example - this complementarity arises from stable regional climatic regimes, where clear-sky solar irradiance peaks during daytime, while moderate-to-strong winds intensify from late afternoon through the night [3], [33], [39], [44]. These conditions align naturally with the operational envelope of VIV-based bladeless turbines, whose oscillatory behaviour is well adapted to turbulent boundary-layer wind regimes characteristic of desert environments [12], [22].

Recent solar resource assessments show that Morocco records some of the world's highest global horizontal irradiation (GHI) values, frequently exceeding 2,000 $kWh \cdot m^{-2} \cdot yr^{-1}$ in its southern provinces [3], [4], [6], [44], [45], [46], [47], [48]. Despite this abundance, photovoltaic output remains constrained by diurnal cycles, temperature-induced derating effects, cloud transients, and angular losses [2], [49], [50]. In contrast, Saharan wind regimes tend to peak several hours after maximum irradiance, driven by land-sea temperature gradients and late-day boundary-layer dynamics [39], [51]. This systematic time shift forms the physical basis of hybridization strategies: when PV output declines at sunset or becomes null at night, wind generation - particularly from devices operating efficiently at low-to-moderate wind speeds - can maintain a useful share of renewable supply.

Because VBTs operate optimally between 3 and 8 $m \cdot s^{-1}$ [12], [19], [23], [52], they are well matched to evening Saharan winds, which often fall below the rated speeds of conventional horizontal-axis wind turbines (HAWTs). Complementarity studies based on residual-load metrics [51], dedicated indices [39] and joint probability distributions [40], [53] consistently report negative correlations between irradiance and wind speed across arid climates. In southern Morocco, Hajou et al. [39] observed diurnal complementarity with SWCI values approaching -0.7, while Meister et al. [40] demonstrated that combined PV-wind operation reduces short-term ramping events and mitigates pressure on storage systems.

From an engineering perspective, hybridization further enhances the suitability of VBTs for microgrid deployment. Their compact and quiet architecture enables installation within PV fields without producing shading effects [13], [20], [54]. Their oscillatory structures create minimal wake interactions, allowing denser layouts than rotating turbines [17], [26], [27]. Furthermore, their smooth aerodynamic response contributes to improved voltage stability in converter-dominated microgrids [35], [52], [55]. Several hybrid-microgrid studies report that combined PV-wind operation can reduce storage requirements by approximately 20–45%, depending on climatic conditions [8], [9], [56], [57].

Spatial complementarity is also significant. The Moroccan Sahara combines exceptional solar potential with coastal and desert wind corridors shaped by Atlantic trade winds and mesoscale convection [3], [11], [33], [39]. This overlap simplifies hybrid system siting and strengthens rural electrification initiatives, as demonstrated in case studies from Morocco and analogous regions [34], [7].

Overall, the complementary behaviour of solar and wind resources provides a strong conceptual basis for integrating VBT clusters into decentralized renewable infrastructures. The synergy between high daytime irradiance and evening/night-time wind availability supports smoother renewable generation, improved voltage stability, and more resilient microgrid operation under Saharan climatic constraints.

2.1. Climatic and Temporal Drivers of Complementarity in the Moroccan Sahara

The Atlantic Sahara exhibits a pronounced diurnal anti-correlation between irradiance and wind speed, which is central to hybrid energy planning. Solar irradiance follows a well-defined unimodal curve under clear-sky conditions, with peak GHI occurring around solar noon. In contrast, wind velocities typically rise several hours later, reaching their maximum from late afternoon through midnight. These atmospheric patterns stem from land–sea temperature gradients, convective cycles, and desert boundary-layer dynamics [3], [45], [58], [59].

Such time-shifted behaviour creates highly favourable conditions for hybrid renewable operation: photovoltaic systems dominate generation between 10:00 and 16:00, while winds of approximately 5–8 $m \cdot s^{-1}$ prevail during evening hours. These wind speeds fall squarely within the lock-in operating range of VBTs [23], [52], [54], thereby reinforcing their functional compatibility with solar-based generation systems.

Complementarity analyses based on correlation metrics, dedicated indices, and residual-load modelling consistently classify the Moroccan Sahara among the regions exhibiting the strongest natural synergy between solar and wind resources [39], [40], [51]. These insights form the scientific and operational foundation for the PV–VBT co-integration explored in this review, particularly in the Boujdour case study.

2.2. Hybrid PV-VBT Complementarity: Semi-Quantitative Energy Assessment

A semi-quantitative analysis was conducted to translate complementarity patterns into operational terms using environmental conditions representative of Boujdour. This evaluation provides an initial validation layer and establishes a transition toward the modelling framework introduced in Section 6.4.

Figure 1 presents normalized hourly power profiles for a 20 kW PV array and a ten-unit VBT cluster under clear-sky spring conditions. The PV system peaks near 1.0 p.u. around midday before declining rapidly after sunset - behaviour consistent with thermal derating and angle-of-incidence losses observed in desert PV installations [2], [4]. By contrast, VBT output increases during late afternoon and evening, when coastal winds intensify due to atmospheric pressure gradients. Evening wind speeds of 6.5 ± 1.2 $m \cdot s^{-1}$ yield aggregated VBT outputs of approximately 0.30–0.38 kW for the micro-turbine configuration considered.

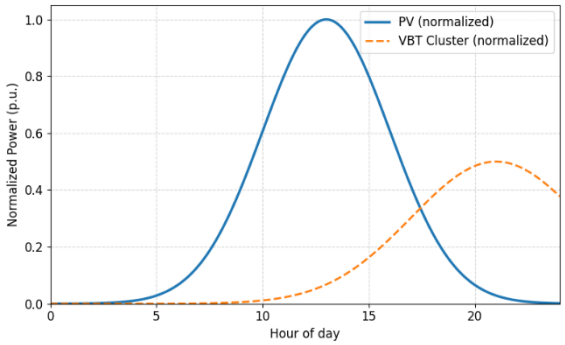

Figure 1. Normalized Daily Power Profiles of PV and VBT Subsystems

Daily energy yields confirm this trend. Under standard conditions, the 20 kW PV subsystem produces approximately 108–122 $kWh \cdot day^{-1}$ [3], [6], [44], [47], [48], [58], while the VBT cluster provides approximately 3.8–5.2 $kWh \cdot night^{-1}$. Although modest relative to PV generation, this nighttime contribution improves operational continuity by smoothing the renewable generation profile and reducing storage usage - effects consistently reported in hybrid microgrid studies under comparable climatic conditions [8], [19], [42].

Table 1 compares the key characteristics of both subsystems. PV generation dominates overall output, while VBTs provide a strategically timed complementary contribution during periods of zero solar availability, thereby supporting continuous renewable operation in desert microgrids.

Table 1. Comparative Characteristics of the PV Array and VBT Cluster

Parameter	**PV Subsystem (20 kW Array)**	**VBT Cluster (10 Units)**	**Remarks**
Primary Resource	Solar irradiance (GHI)	Near-surface wind speed	Distinct climatic drivers ensure temporal complementarity
Peak Period	Midday (12:00-14:00)	Evening-night (18:00-24:00)	Negative correlation between resources (≈ -0.6 to -0.7 in Sahara)
Power Profile (p.u.)	Sharp Gaussia	Broad turbulent-	Figure 1 shows

	n-like peak	driven plateau	normalized profiles
Typical Output	108-122 kWh.day^{-1}	3.8-5.2 kWh.day^{-1}	VBT contribution ≈ 3-4% of PV generation
Sensitivity to Environment	Strongly affected by high temperature, dust, angle-of-incidence	Weak sensitivity to temperature and sand abrasion	VBTs benefit from absence of rotating blades
Typical Operating Range	Controlled by irradiance cycles	Efficient between 3-8 m·s^{-1}	Saharan evening winds fall within VBT optimal zone
Variability	High diurnal intermittency	Lower short-term intermittency	Oscillatory VIV response smooths microgrid voltage
Maintenance Profile	Seasonal cleaning + thermal derating checks	Very low (no blades, low mechanical wear)	Advantageous for desert hybrid microgrids
Contribution to Microgrid Stability	Dominant daytime supply	Supports evening/night renewable continuity	Reduces storage cycling depth
Spatial Footprint	High land occupation for array	<3% of PV site footprint	Co-location possible without shading
Hybrid Benefit	High energy yield	Reinforces nighttime renewable availability	Hybridization reduces storage needs by 20-45%

This preliminary assessment constitutes a structured validation step for PV–VBT co-integration under Saharan conditions. It supports the expanded Boujdour case study presented in Section 6.4 and demonstrates the practical relevance of hybrid renewable architectures for desert microgrid applications.

To fully exploit this hybrid potential, a rigorous understanding of the underlying VIV physics is required. This naturally motivates the detailed examination of vortex-induced vibration mechanisms presented in Section 3.

3. Physics of Vortex-Induced Vibrations (VIV)

Vortex-induced vibrations (VIV) constitute the fundamental operating principle of vortex bladeless turbines (VBTs). When a slender bluff body - typically a cylindrical or tapered mast - is exposed to an airstream, alternating Bénard-von Kármán vortices form on either side of the structure, generating a transverse fluctuating lift force. This unsteady aerodynamic loading excites the mast and produces mechanical oscillations suitable for energy harvesting. Maximum efficiency is achieved when the vortex-shedding frequency f□ approaches the structural natural frequency f_n , thereby establishing a lock-in regime in which oscillations become synchronized and self-sustained [12], [14], [15], [24], [60].

The shedding frequency follows the classical Strouhal relation:

$$f_s = S_t \cdot \frac{V}{D} \quad (1)$$

where V denotes the free-stream velocity, D the characteristic mast diameter, and $S_t \approx 0.18\text{-}0.22$ for circular cylinders in the subcritical Reynolds regime. Numerous experiments confirm the robustness of this proportionality and its sensitivity to geometric slenderness, taper ratio, and surface roughness [24], [34], [37], [60], [61]. Lock-in typically arises when f□ ≈ f□ for Reynolds numbers in the range 10^3-10^5, where coherent shedding persists despite emerging three-dimensional instabilities [35], [62].

Extensive CFD–FSI and reduced-order studies show that lock-in is intrinsically nonlinear, exhibiting amplitude saturation, hysteresis, and a marked dependence on structural damping ζ, mass ratio m□, and effective stiffness [15], [25], [26], [37]. At low Reynolds numbers, the oscillations remain quasi-harmonic, whereas higher values trigger vortex dislocations, mode switching, and increased wake three-dimensionality [35], [36], [37]. Reduced-order

wake-oscillator models (e.g., modified Van der Pol formulations) reliably capture these behaviors by coupling hydrodynamic forcing with structural displacement and velocity [10], [15], [34]. Their predictions are broadly consistent with high-fidelity CFD–FSI simulations, which provide detailed insight into stability envelopes and oscillation amplitudes [63], [64], [65].

3.1. Influence of Geometry, Damping, Mass Ratio, and Material

From a design perspective, the dynamic response of a VBT is governed primarily by its geometry, damping, material stiffness, and mass distribution. These interdependent parameters control the onset of lock-in, the achievable amplitude, and the overall stability of oscillations. Table 2 summarizes their principal effects based on recent experimental and optimization studies.

Table 2. Influence of Key Parameters on VBT Dynamic Response

Design Parameter	Physical Effect	Design Implication for VBTs	Reference
Geometry (D, taper ratio)	Sets Strouhal number (St), wake stability, and vortex spacing	Determines lock-in bandwidth and amplitude response	[10], [21], [24], [34], [66], [67]
Damping ratio (ζ)	Controls energy dissipation and stability margin	Must balance oscillation amplitude growth and resonance sustainment	[15], [25], [26]
Mass ratio (m^*)	Influences fluid–structure coupling strength and sensitivity	Low (m^*) enhances lock-in; excessively low values may induce instability	[14], [15], [37]
Material properties (E/ρ)	Define stiffness-to-mass ratio and natural frequency (f_n)	Composite materials can extend lock-in to higher wind-speed regimes	[15], [21], [24], [68]

The balance among these parameters is critical. Excessive stiffness or damping suppresses oscillatory amplitude, while overly compliant structures may develop irregular trajectories or premature fatigue, a failure mode frequently reported in VIV harvesters [18].

3.2. Lock-in Dynamics and Phase Synchronization

Figure 2 illustrates the synchronized evolution of vortex shedding and structural displacement during lock-in. Energy transfer efficiency is controlled by the phase relation between transverse velocity and lift force: near-perfect synchronization maximizes extracted mechanical work, whereas phase deviation reduces effective coupling.

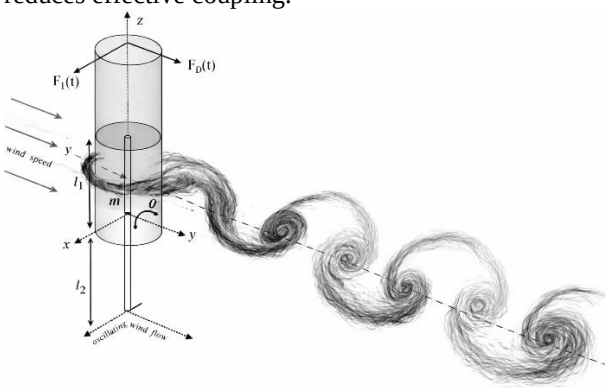

(a)

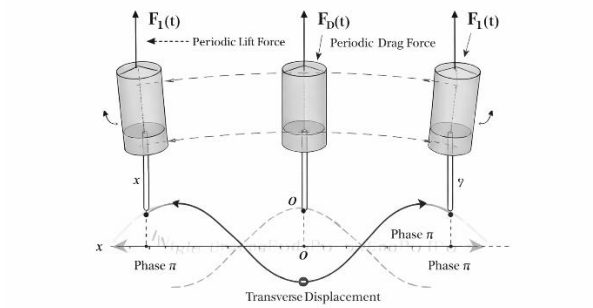

(b)

Figure 2. (a):Phase-Locked Vortex Shedding During Lock-In; (b): Phase-Synchronized Structural Displacement During Lock-In

Across multiple studies, slender or tapered geometries maintain a mean Strouhal number of approximately 0.20 ± 0.02, supporting stable lock-in within reduced-velocity ranges: $U^* = \frac{V}{f_n D} \approx 4 - 10$, as reported in [24], [35], [37], [62]. Tapered profiles

can widen the synchronization bandwidth by up to 25 %, a significant advantage for compact or densely arranged VBT arrays [28]. Conversely, increasing structural damping narrows the lock-in window, and excessive tapering may destabilize the wake.

These effects are particularly important for hybrid solar-wind microgeneration: achieving reliable lock-in at low-to-moderate wind speeds (2-9 $m \cdot s^{-1}$) directly supports evening-nighttime complementarity with PV systems in desert microgrids [39], [69].

3.3. Governing Physical Principles for VBT Design

Table 3 consolidates the dominant physical mechanisms driving VIV energy harvesting and their implications for practical VBT design.

Table 3. Summary of Physical Principles Governing VBT Design

Phenomenon	Dominant Parameter	Effect on Performance	Design Guideline
Vortex shedding frequency	$St \cdot \frac{V}{D}$	Controls lock-in initiation	Match $f_n \approx f_s$ for broad, stable bandwidth
Damping hysteresis	Structural ζ	Shapes stability envelope	Maintain $\zeta \approx 0.01$-0.05
Mass ratio	$M^* = \frac{\rho_s}{\rho_f}$	Determines oscillation strength	Intermediate values (10-20) give optimal coupling
Geometric taper	Shape gradient	Adjusts vortex spacing, wake stability	Positive taper reduces interference and widens lock-in

Together, these relationships show that optimal performance arises from carefully balancing aerodynamic excitation, structural flexibility, and wake coherence. A properly tuned turbine maintains a stable synchronized response across realistic wind conditions, making VBTs particularly suitable for supplementing photovoltaic generation in arid and semi-arid regions.

4. Engineering Framework of Vortex Bladeless Turbines (VBTs)

A vortex bladeless turbine consists of a slender cantilevered mast - cylindrical or conical - whose transverse oscillations are driven by unsteady aerodynamic forces originating from vortex shedding. Its operation relies on maintaining resonance between the structural natural frequency and the vortex-shedding frequency within the Strouhal band defined in Eq. (1), while ensuring structural durability under realistic atmospheric variability [12], [14], [23], [24], [31]. Unlike horizontal-axis wind turbines equipped with blades, hubs and gearboxes, the VBT architecture suppresses rotating assemblies, resulting in a silent, lightweight and low-maintenance system suitable for urban sites, microgrids and hybrid decentralized generation in regions such as North Africa [13], [20], [61], [70], [71].

The aerodynamic loads acting on the mast include both lift and drag contributions. The instantaneous lift forcing the transverse oscillation is expressed as

$$F_L(t) = \frac{1}{2}\rho V^2 C_L(t) A \quad (2)$$

where A denotes the projected frontal area, while the mean drag load is

$$F_D = \frac{1}{2}\rho V^2 C_D A \quad (3)$$

with C_D typically ranging from 1.1 to 1.3 for circular cylinders in subcritical flow [24], [38], [63], [72].

The mast behaves as a damped oscillator subjected to the unsteady lift:

$$m\ddot{x}(t) + c\dot{x}(t) + kx(t) = F_0 cos(\omega t) \quad (4)$$

with natural frequency and damping ratio

$$f_n = \frac{1}{2\pi}\sqrt{\frac{k}{m}} \quad (5)$$

$$\zeta = c2km \quad (6)$$

Resonance (lock-in) is achieved when the shedding frequency f_s approaches f_n, enabling stable large-amplitude oscillations and efficient mechanical energy extraction [12], [24], [31], [52], [62], [73].

The instantaneous mechanical power harvested from wind forcing is

$$P_{mech}(t) = F_L(t)\,\dot{x}(t) \quad (7)$$

and the average harvested power over a vibration period is:

$$\bar{P}_{mech} = \frac{1}{2}\rho A C_L V^2 \overline{\dot{x}(t)} \quad (8)$$

Experimental and CFD-FSI results consistently show lock-in ranges between 2 and 8 $m \cdot s^{-1}$ for slenderness ratios below 30, defining the practical scalability limits for VBT deployment [15], [24], [28], [31], [37], [74].

4.1. Structural tuning and parametric influence

The key design parameters - mass m, stiffness k and damping c - govern the oscillation amplitude, lock-in bandwidth and vibrational stability. Their influence is summarized in Table 4.

Table 4. Parametric influence of m, k, and c on VBT resonance behavior

Parameter	Physical Effect	Design Role	Reference
m	Inertia, frequency shift	Controls spectral width and stability	[24], [25], [31], [75]
k	Structural stiffness	Tunes f_n within Strouhal band	[23], [24], [60], [66], [76]
C	Energy dissipation	Stabilizes oscillation amplitude	[18], [25], [54], [77], [78]

Maintaining $f_n \approx f_s$ under fluctuating wind requires adaptive tuning strategies. Recent prototypes integrate movable sleeves, variable-stiffness inserts or tunable inertial masses that modify k and m in real time, extending the operational lock-in range while controlling fatigue [21], [23], [27], [29], [76], [79].

Figure 3 illustrates such an adaptive configuration, where combined stiffness- and mass-tuning mechanisms achieve resonance across low-to-moderate winds (2-9 $m \cdot s^{-1}$), a critical requirement for urban and microgrid applications [23], [29], [76].

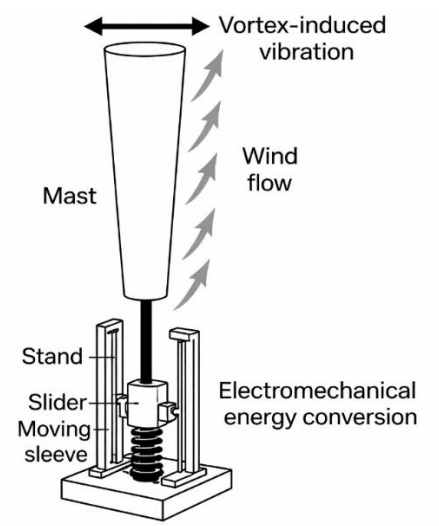

Figure 3. Adaptive VBT with variable-mass system

The amplitude-wind response predicted from Eq. (7), and depicted in Figure 4, confirms that moderate damping and intermediate stiffness maximize resonance plateaus, enabling stable operation across broad wind ranges. Similar results are reported in numerical and experimental analyses of VBTs and VIV energy harvesters [17], [31], [37], [73], [74].

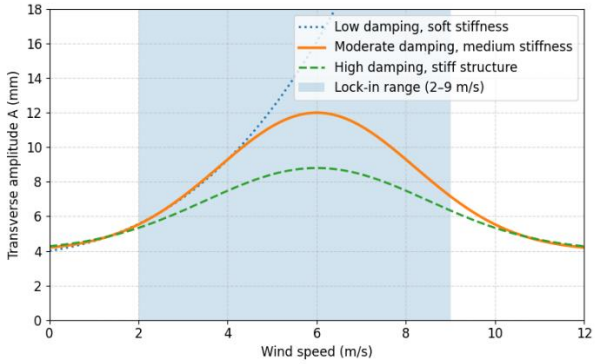

Figure 4. Resonance behavior of a vortex bladeless turbine under varying damping and stiffness conditions

4.2. Nonlinear dynamics and design-space considerations

Design-space optimization shows that even modest adjustments in stiffness or damping may considerably increase lock-in duty cycles and net harvested energy under unsteady winds [4], [10], [17], [73]. Reduced-order models - including modified Van der Pol oscillators, wake-oscillator formulations and multi-mode nonlinear systems [24], [38], [52], [74], [80], accurately reproduce key nonlinearities such as hysteresis, saturation and phase-locking. Their predictions agree with high-fidelity CFD-FSI simulations [21], [36], [72], [81], [82].

4.3. Material considerations

Material selection determines stiffness-to-mass ratios, damping properties, fatigue life and environmental resistance. Composite structures (carbon-fiber, epoxy-glass, hybrid laminates, thermoplastic sandwich skins) are widely adopted in current VBT prototypes due to their advantageous mechanical properties [19], [21], [54], [67], [83]. Table 5 consolidates the main design-oriented material criteria.

Table 5. Material selection criteria for VBT structures

Criterion	Design Implication	Example Materials	Reference
High E/ρ	Increases f_n without mass penalty	Carbon-fiber composites	[19], [21], [83]
Moderate damping ($\zeta = 0.02$-0.05)	Ensures stable lock-in	Hybrid laminates	[24], [67], [77], [21].
High fatigue strength	Extends life beyond 5 years	Epoxy-glass	[18], [54], [67]
Recyclability	Improves environmental metrics	Thermoplastics	[22], [67]

4.4. CFD-FSI modeling and experimental validation

The aero-structural behavior of VBTs is governed by nonlinear fluid-structure interactions. Two-way CFD-FEM coupling - using URANS, LES, particle-vortex methods and ALE dynamic meshing - is widely adopted to capture vortex shedding, wake-structure synchronization and pressure-load evolution [21], [25], [36], [38], [62], [81], [84].

This self-sustained feedback loop is summarized in Figure 5 and mirrors the canonical behavior of VIV harvesters [74], [85], [86], [87].

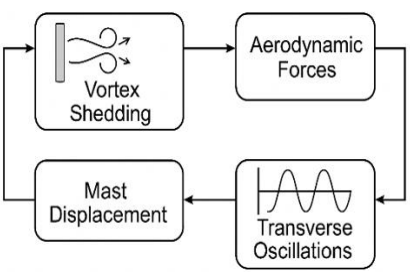

Figure 5. self-sustained FSI loop

Experimental validations - via wind-tunnel tests, prototype deployments and multimodal sensing (accelerometers, optical encoders, high-frequency DAQ) - confirm the predictive accuracy of these modeling strategies and validate the performance gains of stiffness-tuning and resonance-shifting modules [23], [29], [31], [54], [79], [88].

4.5. Remaining challenges

Despite these advances, several scientific and engineering challenges persist:

- modeling of large-amplitude nonlinearities and multi-mode interactions [38], [74], [75];
- realistic representation of atmospheric turbulence and desert boundary-layer effects [89];
- limited long-term datasets on composite-joint aging and fatigue beyond five years [18], [54], [67];
- absence of standardized design and certification frameworks specific to VBTs [85], [90], [91].

Progress toward scalable, certifiable VBT technologies will require hybrid workflows combining reduced-order and CFD-FSI models, standardized testing protocols, and extended durability studies under real-world conditions [10], [23], [24], [90].

5. Performance Assessment of Vortex Bladeless Turbines

The performance of vortex bladeless turbines (VBTs) results from the coupled aerodynamic, structural, and electromechanical mechanisms that govern their vortex-induced vibration (VIV) energy-harvesting process. Unlike rotational wind machines, VBTs operate within a resonance-dominated regime, making their performance metrics highly sensitive to unsteady inflows and turbulence. To ensure comparability with conventional small-wind systems, the power coefficient remains the primary performance indicator, defined as:

$$C_p = \frac{P_{electrical}}{\frac{1}{2}\rho A V^3} \quad (9)$$

where $P_{electrical}$ is the rectified electrical output, ρ\rhoρ the air density, V the wind speed, and A the effective frontal area encompassing the vibrating mast and its near-wake region [12], [14], [10]. Performance characterization typically follows IEC 61400-2 procedures, including cut-in velocity, rated operating point, acoustic levels, and measurement uncertainty [90].

Because VBTs operate through oscillatory motion rather than continuous rotation, several complementary metrics are required in addition to C_p. These include the cut-in velocity V_{ci}, the lock-in duty factor (fraction of time spent within the resonance band), the resonance-tracking efficiency under gusts, the electromechanical conversion efficiency (piezoelectric or electromagnetic), acoustic

emissions, and fatigue-related indicators such as amplitude-to-diameter ratio and vibration-cycle count to failure [20], [21], [22], [67].

Although VBTs generally exhibit lower absolute C_p values than horizontal- or vertical-axis turbines of similar scale, they offer advantages in acoustic performance, mechanical simplicity, and deployability in dense or constrained environments [13], [14], [16]. Measurements on representative 3-m prototypes indicate cut-in speeds of 2-3 $m \cdot s^{-1}$ and peak outputs of 80-120 W at 8-9 $m \cdot s^{-1}$, supported by wind-tunnel tests and outdoor trials [12], [29], [70].

Scaled laboratory models produced using additive manufacturing reproduce the essential lock-in behavior and vortex-synchronization mechanisms. High-resolution laser vibrometry and instrumented electromagnetic harvesters provide synchronized displacement-frequency-voltage measurements that support model identification and dynamic characterization [19], [70].

Performance improvements are closely linked to adaptive tuning strategies aimed at maintaining the natural frequency f_n within the Strouhal band despite fluctuating winds. Techniques such as adjustable stiffness modules, tunable inertial masses, and sliding sleeves have proved effective in stabilizing oscillation amplitudes and extending the lock-in bandwidth [27], [85], [92]. The use of composite or sandwich materials further enhances stiffness-to-mass ratios and damping characteristics, improving resonance stability and fatigue resistance [21], [54], [67].

Wind-tunnel investigations remain essential for isolating Reynolds-number and turbulence effects on VBT response. Numerical and experimental studies - such as those by Canilho et al. - show strong agreement between CFD predictions and frequency responses in elastically mounted cylinders [24]. Additional work confirms that nonlinear stiffness elements can enlarge the lock-in region and enhance energy extraction under moderate winds [70].

Field measurements introduce additional variability due to gustiness, vertical shear, and diurnal atmospheric stratification. Devices that incorporate self-calibrating inertial masses or discrete resonance-shifting mechanisms exhibit improved phase synchronization under fluctuating inflows, which reduces output variance and increases cumulative yield [27], [92]. Outdoor trials in arid and semi-arid climates further indicate that, once properly calibrated, deviations between modeled and measured outputs remain narrow [27], [29], [54]. Recent techno-economic and environmental assessments also support the feasibility of deploying VBTs in hybrid renewable systems [2].

Unlike conventional turbines, where torque fluctuations propagate through gearboxes and drivetrains, VBTs follow a damping-dominated dynamic behavior. High-frequency perturbations are naturally filtered by structural and electromechanical damping, which stabilizes power output in the lock-in plateau and limits fatigue stresses [10], [15], [62].

Figure 6 summarizes the frequency-response and power-spectrum characteristics, illustrating synchronization between the vortex-shedding frequency f_s and the structural natural frequency f_n. Combined CFD-FSI simulations and wake-oscillator models consistently show that moderate damping and appropriate stiffness-to-mass ratios maximize vibrational energy harvesting under transient wind conditions [10], [15], [62].

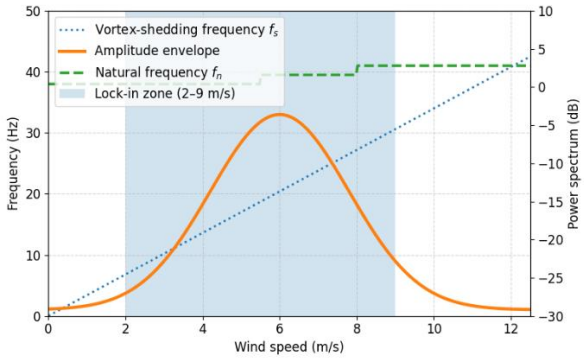

Figure 6. Frequency-response and power spectrum of the VBT showing lock-in synchronization between vortex-shedding and structural frequencies

Figure 7 presents the time-domain dynamics in the lock-in regime, highlighting the synchronized evolution of tip displacement and lift force. The strong amplitude-phase correlation characteristic of stable resonance offers valuable insight for defining thresholds and control rules for adaptive tuning mechanisms [34].

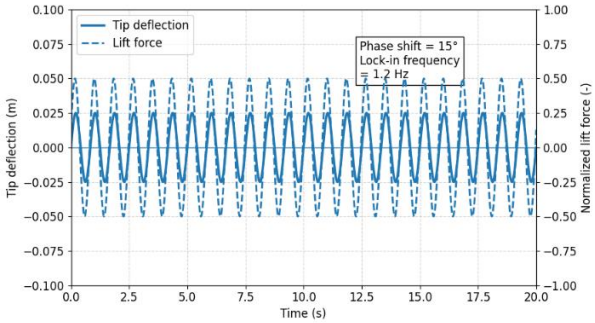

Figure 7. Simulated lock-in regime of a VBT showing synchronized tip deflection and lift force (conceptual data from [34])

To complement this analysis, Table 6 provides a functional benchmarking matrix comparing HAWTs, VAWTs, and VBTs. Rather than relying on nominal efficiencies, the comparison emphasizes practical trade-offs involving acoustic compliance, mechanical complexity, deployment density, and suitability for hybrid PV-wind microgrids. While VBTs exhibit modest C_p, they provide unique advantages, minimal noise, simple structure, and effective integration in densely populated or spatially constrained areas [37], [49], [50].

Table 6. Comparative functional benchmarking of small-scale wind technologies.

Criterion	**HAWT**	**VAWT (Darrieus / Savonius)**	**VBT**	**Updated Representative Sources**
Aerodynamic regime	High lift-torque; yaw-sensitive	Mixed lift-drag	Transverse oscillatory lift (VIV)	[14], [16], [23], [38]
Operating wind range (m s^{-1})	3-25 ; optimal > 6	2-18	2-9 (lock-in band)	[12], [23], [29], [54].
Resonance / Control strategy	Active pitch-yaw	Passive or vane-guided	Adaptive stiffness/ mass tuning & resonance shifting	[27], [29], [35], [76].
Mechanical complexity	Rotor, gearbox, bearings	Moderate	Very low (no rotor)	[12], [10], [37], [13].
Acoustic & environmental footprint	45-60 dB; bird-strike risk	40-55 dB	< 35 dB; no rotating blades	[13], [23], [28], [49]
Maintenance intensity	Frequent lubrication & alignment	Periodic	Minimal (structural check)	[12], [13], [37]
Spatial footprint / areal power density	Large spacing due to strong wakes	Moderate spacing	Compact arrays; weak wakes	[23], [31], [37], [50]
Typical applications	Utility-scale farms	Small off-grid / rural rooftops, PV-hybrid	Urban microgrids,	[31], [33], [42], [49], [50],

From a system perspective, VBTs align well with hybrid solar-wind microgeneration strategies, particularly where nocturnal winds complement daytime solar availability. Their low acoustic impact and minimal mechanical complexity facilitate seamless integration into urban and off-grid microgrids [33], [37]. Nevertheless, rigorous performance benchmarking still requires LCOE normalization and uncertainty quantification in accordance with IEC 61400-2 [14], [31], [90].

Accordingly, a comprehensive evaluation framework should combine:

- reduced-order models (modified Van der Pol, wake-oscillator with saturation);
- CFD-FSI simulations (URANS/LES) to resolve near-wake dynamics;
- instrumented prototypes capturing synchronized electromechanical and kinematic data [10], [15], [24], [25], [26], [62];
- fatigue and depolarization tracking for piezoelectric systems [22];
- precise assessment of electromagnetic losses and cogging torque in generator-based designs [12], [20], [27].

Despite substantial progress, key challenges remain. Long-term durability data - particularly beyond five years - are still limited for composite joints and mast-base assemblies [21], [22], [54], [67]. Scaling laws for transitioning from laboratory devices to multi-kilowatt units require further validation, especially for C_p , damping behavior, and electromagnetic characteristics [10], [66]. Moreover, standardized acoustic qualification and site-specific validation procedures must be developed to ensure technological bankability [14], [90].

Because VBT performance is highly sensitive to atmospheric conditions, combined numerical-experimental assessment remains indispensable prior to deployment, particularly in urban canyons, coastal locations, and desert sites [28], [30], [31].

In summary, although VBTs exhibit lower aerodynamic efficiency than classical turbines, their adaptive resonance behavior, low mechanical complexity, and minimal acoustic signature position them as promising low-impact wind harvesters. Their competitiveness will increasingly depend on durability-centered design, advanced tuning strategies, and standardized validation frameworks - critical enablers for future integration in solar-dominated hybrid microgrids and decentralized energy systems.

6. Control, Deployment Optimization and Sustainable Integration

The operational reliability of vortex bladeless turbines (VBTs) depends on maintaining stable resonance, protecting structural components from fatigue, and ensuring efficient energy extraction under fluctuating wind conditions. These requirements call for coordinated control strategies spanning the device scale, the cluster scale, and the system-integration level within hybrid PV-wind microgrids.

6.1. Adaptive Resonance Control

Modern VBTs incorporate multi-layer control architectures combining passive, semi-active, and low-power active mechanisms. Passive elements - nonlinear elastic supports, orthotropic composite masts, and guided inertial masses - allow autonomous adjustments of the stiffness-to-mass ratio, enabling the system to remain close to its natural frequency without external energy consumption [12], [27], [85], [92]. Semi-active damping modules, typically magneto-rheological or electromagnetic, increase the effective lock-in bandwidth with minimal power overhead [76]. When rapid corrections are required during gusts, lightweight active devices such as sliding sleeves or piezoelectric micro-adjusters provide fine real-time tuning, stabilizing oscillation amplitude and enhancing electromechanical conversion efficiency [27], [92].

Figure 8 (reproduced from the experimental architecture developed in this study) illustrates this layered control logic. Local sensors monitor mast deflection and vibration frequency; a semi-active electromagnetic damping stage regulates the oscillatory envelope; and an adaptive stiffness/mass-tuning module maintains the convergence between structural and shedding frequencies. A supervisory controller integrates these signals and exchanges set-points with the reinforcement-learning optimization layer, enabling predictive adjustment of k, c, and D/D ratios and ensuring robust resonance tracking within hybrid microgrid operation.

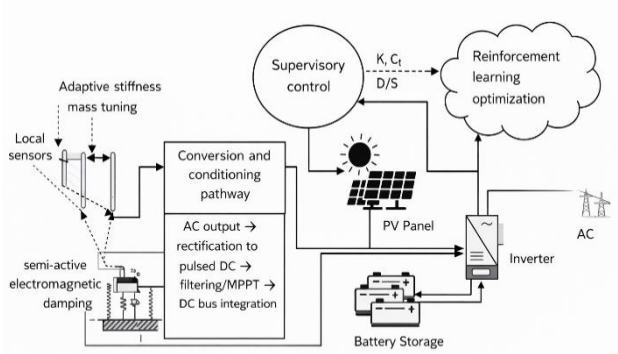

Figure 8. Integrated control and deployment Architecture of a VBT cluster within a hybrid PV-wind microgrid

6.2. Cluster-Level Optimization and Wake Coordination

At the deployment scale, cluster dynamics are governed by inter-device coupling, wake interactions, and the spatial distribution of turbulent energy. VBTs generate compact, low-intensity wakes that dissipate rapidly relative to those of HAWTs or VAWTs, enabling dense layouts in confined sites such as rooftops, peri-urban zones, and PV fields [12], [13], [23].

To exploit these properties, several optimization approaches - including Particle Swarm Optimization (PSO), Ant Colony Optimization (ACO), and hybrid metaheuristics - have been extended to VBT arrays. These methods integrate wake-oscillator surrogates [10], turbulence-induced phase coupling [31], acoustic-compliance constraints [23], and structural-stability criteria. Reinforcement-learning controllers have also demonstrated the ability to adjust spacing, activation sequences, and tuning parameters in real time under turbulent inflows [14], [31].

Table 7 summarizes the principal optimization variables and expected performance improvements. Typical gains include up to +20% power-per-area from optimized spacing, +15% increase in lock-in duty through stiffness tuning, reduced fatigue amplitude under electromagnetic damping, and modest but consistent yield improvements through resonance-tracking control.

Table 7 summarizes the main control and layout parameters, along with expected performance gains

Parameter	Objective	Method	Expected Gain	Reference
Normalized spacing (S/D)	Maximize areal power density	Wake-oscillator surrogate	+20% power/area	[17], [23], [26],
Stiffness (k)	Broaden lock-in band	Passive + active tuning	+15% lock-in duty	[28], [52], [76].
Damping (c)	Stabilize oscillations	Electromagnetic feedback	−30% fatigue amplitude	[10], [62], [77]
Tracking ($f_n \rightarrow f_s$)	Maintain resonance	Sliding-mass control	+10% energy yield	[29], [65], [23].

6.3. Integration within Hybrid PV-Wind Microgrids

VBTs complement PV systems by providing renewable energy during evening and nocturnal periods when solar output falls to zero. Their rotor-less architecture eliminates the acoustic and mechanical constraints associated with rotating blades and simplifies integration into hybrid microgrids [12], [13], [49]. Because VBTs deliver rectified DC power, they interface naturally with standard droop-controlled converters, SoC-window algorithms, and low-inertia stabilization schemes used in remote microgrids [50], [93].

This additional nocturnal contribution reduces reliance on storage and moderates battery cycling, particularly in Saharan regions where evening wind intensification is well documented [2], [13], [23], [39]. Composite and sandwich-material masts with high stiffness-to-mass ratios increase durability under desert winds, while the absence of rotating components minimizes sand-induced degradation [21], [54], [67].

6.4. Case Study: Boujdour PV-VBT Hybrid Microgrid

To validate the hybrid architecture, an experimental arrangement was deployed at the Boujdour site. Figure 9 shows the test configuration: a 330 Wc PV module inclined at 25°, two micro-scale VBTs of 2 m height spaced at 0.8 m, an irradiance sensor delivering G(θ,t), a meteorological mast equipped with cup-anemometers, and two energy loggers connected to the 48 V DC microgrid bus.

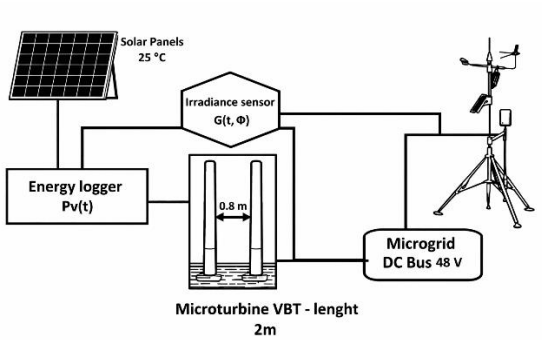

Figure 9. Hybrid PV-VBT experimental arrangement

Boujdour, located along the Atlantic façade of the Moroccan Sahara, combines high solar potential (GHI > 2000 kWh·m^{-2}·yr^{-1}) [3], [6], [33], [44], [45], [47], [48], [58]. with stable evening winds driven by coastal thermal gradients [11]. These winds typically reach 5-8 m·s^{-1} during late-afternoon and nighttime periods - well aligned with the operational envelope of VIV-based turbines [12], [23], [28], [52].

The case study considers a 20 kW PV array coupled with a 10-unit VBT cluster deployed on a compact 200-300 m² area adjacent to the PV field. The VBT array uses staggered spacing of approximately 4-5 diameters, consistent with VBT wake-attenuation studies [17], [26], [27]. Under evening winds of 6.5 ± 1.2 m·s^{-1}, the cluster delivers approximately 280-380 W, providing a stable nocturnal input that mitigates short-term variability and reduces early battery discharge. Similar configurations have been validated in rural and peri-urban electrification projects across Morocco and comparable regions [7], [34], [56].

From a power-quality standpoint, VBTs generate smoother DC output than conventional small wind turbines due to their intrinsic damping-moderated oscillatory response, thereby improving DC-bus stability in converter-dense microgrids [93], [94]. Their resistance to sand abrasion further enhances durability in Saharan conditions [5], [89].

Because VBTs occupy < 3% of the PV site footprint and do not cast significant shadows, they can be co-located within PV fields without reducing solar yield. In this configuration, the addition of ten VBTs increases annual renewable production by 2.5-3.0% and reduces diesel runtime, lowering the LCOE of hybrid installations [105-109], [128].

6.5. Environmental Robustness and Long-Term Sustainability

Life-cycle assessments indicate that VBTs generally possess lower embodied energy and greenhouse-gas emissions than small HAWTs due to their simplified mechanics and restricted material use [12], [13], [14]. Composite coatings, sealed housings, and corrosion-resistant alloys preserve functionality under harsh desert, coastal, or high-salinity conditions [21], [54], [67].

Robust techno-economic assessment requires the adaptation of IEC 61400-2 to VBT-specific characteristics, including effective-area definition, turbulence metrics, acoustic compliance, electromagnetic compatibility, and durability testing [14], [90]. Although existing prototypes show encouraging fatigue performance, long-term endurance datasets beyond five years remain limited for composite joints and mast-base interfaces [21], [22], [54], [67].

6.6. Toward Intelligent, Self-Regulated Micro-Wind Architectures

Combining adaptive control, optimal cluster deployment, and PV-wind hybrid integration leads to intelligent VBT modules capable of autonomously sustaining resonance. Figure 8 captures this closed-loop interaction: aerodynamic forcing, structural tuning, and power conditioning mutually regulate one another through local sensing, supervisory control, and a reinforcement-learning optimization layer.

These characteristics align VBTs with emerging smart-grid paradigms emphasizing distributed generation, low environmental externalities, and high resilience in regions dominated by strong solar-wind complementarity [37], [39], [51], [95]. Continued progress in structural robustness, adaptive-control algorithms, and standardized validation frameworks will play a critical role in transitioning VBTs from experimental prototypes to fully bankable assets for decentralized renewable-energy systems.

7. Structural Durability, Optimization, and Research Roadmap

The long-term sustainability of vortex bladeless turbines (VBTs) depends on structural resilience, dynamic optimization, and standardized deployment strategies that remain cost-effective at scale [96], [97], [98], [99], [100]. Because mast mechanics, composite materials, resonance-tuning subsystems, power electronics, and hybrid PV-wind coupling interact across multiple physical domains, VBT design must follow a coherent multi-objective engineering framework [101], [102].

The oscillating mast experiences continuous vortex-induced vibrations (VIV), which generate cyclic stresses concentrated near the base and at structural junctions. Reliable lifetime prediction therefore requires fatigue models that combine VIV forcing spectra with multi-axial stress analysis, ideally supported by instrumented monitoring campaigns extending beyond five years [21], [34], [54], [67], [97], [98], [99], [100], [103], [104]. Maintaining modal stability is essential to avoid uncontrolled resonance growth; several studies show that precise stiffness tuning significantly limits fatigue accumulation under turbulent inflows [45], [98], [100]. Composite and sandwich materials offer high stiffness-to-mass ratios and intrinsic damping, helping stabilize vibration amplitudes while delaying crack initiation and propagation [21], [54], [67], [97], [99]. For piezoelectric-based designs, long-term monitoring of depolarization and electromechanical fatigue is required to preserve conversion efficiency [22], [105], [106].

At the farm scale, array performance depends on the interplay between aerodynamic interactions, installation density, and local turbulence levels. Multi-objective optimization frameworks therefore combine turbine-level structural parameters with cluster-level spacing rules. Approaches based on ACO, PSO, or reinforcement learning have shown strong potential for compact deployments, particularly on rooftops or in dense urban environments [30], [31], [52], [120]. Wake-oscillator surrogate models allow rapid exploration of the design space before refinement using high-fidelity FSI simulations [10], [25], [26], [124].

Because resonance stability governs energy extraction, maintaining lock-in across fluctuating winds remains a core operational requirement. Adaptive mechanisms such as discrete resonance shifting, sliding-mass sleeves, guided inertial modules, and hybrid passive-active stiffness control can enlarge the effective lock-in range and mitigate overstress during gusts [17], [27], [35], [76], [101]. When combined with real-time structural health monitoring, these tuning strategies support predictive maintenance and enhance fault tolerance [27], [76].

7.1. Hybrid PV-VBT Durability and System-Level Benefits

In regions where solar production dominates, the durability of VBTs must also be assessed relative to

their functional role within PV-wind hybrid systems. The complementarity between daytime solar generation and nocturnal wind availability tends to reduce battery cycling depth, thereby improving storage lifetime [13], [23], [49], [107], [108], [109], [110], [111]. Their silent, rotor-less operation also facilitates co-location with PV fields on rooftops or façades. Composite coatings and corrosion-resistant alloys reinforce resilience in desert or marine environments [12], [13], [21].

Life-cycle assessment (LCA) studies indicate that VBTs often achieve lower embodied energy and reduced greenhouse-gas emissions compared to small HAWTs of equivalent rating due to simpler mechanics and lighter materials [12], [13], [14]. When integrated into PV-VBT-storage microgrids, the stable nocturnal contribution of VBTs improves the overall capacity factor, reduces PV and battery oversizing, and enhances system resilience [33], [49], [83], [112], [113], [114]. Nevertheless, long-term fatigue datasets - ideally exceeding five years - remain necessary to validate durability under real atmospheric conditions [21], [22], [54], [67].

7.2. Standardization and Techno-Economic Considerations

VBT technology is not yet covered by dedicated certification routes. Adapting IEC 61400-2 to VBT-specific physics - definitions of effective area, turbulence metrics, acoustic thresholds, EMC compliance, durability tests, and power-curve procedures - is crucial for reproducibility, warranties, and bankability [14], [90].

From an economic perspective, competitiveness remains under evaluation. Reductions in the cost of magnets, coils, and lightweight composite materials, coupled with modular and locally manufacturable designs, may improve affordability [14], [63]. However, LCOE must be normalized using consistent parameters, including urban capacity factors, standardized power-curve methods, O&M intervals, and end-of-life scenarios [14], [90], [115], [116], [117], [118], [119]. For hybrid PV-VBT microgrids, nocturnal wind input enhances availability and limits storage requirements [13], [49]. Scaling VBTs to multi-kilowatt ratings introduces new challenges such as stiffness/mass optimization, thermal dissipation in coils, and dispersion of spring fatigue behaviour [10], [17], [66]. Offshore prototypes confirm scalability but require marine-grade materials and survival strategies [15], [28].

Table 8. Comparative synthesis of small HAWT, Darrieus, Savonius, and VBT (unchanged)

Criterion	**Small HAWT**	**Darrieus (VAWT)**	**Savonius (VAWT)**	**VBT (VIV)**
Typical C_p range	0.30-0.45	0.25-0.35	0.10-0.25	Lower C_p (prototype stage)
Cut-in / low-wind behaviour	Moderate cut-in; needs yaw	May struggle to self-start	Excellent self-start	Operable at low winds if lock-in maintained
Yaw sensitivity	High	Moderate	Low	Very low (quasi-omnidirectional)
Acoustic profile	Tonal noise possible	Moderate	Low	Very low (urban-compatible)
Wake strength / spacing	Strong → large spacing	Moderate	Weak	Very weak → high density
O&M complexity	High (rotors, gearbox)	Moderate	Low	Very low (no rotor/gearing)
Grid interface	Standardized	Standard	Standard	Simple DC output
Balance of system	Large tower	Moderate	Simple	Lightweight anchoring
LCOE trend	Mature supply chain	Intermediate	Low CAPEX, low yield	To be standardized
Best-fit use cases	Open, high-wind sites	Steady winds	Rooftops	Urban microgrids, hybrid PV-wind

Across current studies, small HAWTs exhibit the highest C_p under favourable winds, Darrieus turbines show moderate performance but weak self-starting behaviour, and Savonius rotors excel in low-wind regions. VBTs, although less efficient in terms of absolute C_p, offer high simplicity, omnidirectionality, intrinsic safety, and very low acoustic impact,

attributes that make them suitable for urban microgrids, PV co-location, and compact installations [12], [14], [16], [35], [38], [60].

7.3. Research Roadmap

A three-horizon roadmap outlines the steps required to advance VBTs from prototype to standardized micro-wind solutions:

a) Short term (1–3 years)
- Standardized endurance and fatigue campaigns across urban test sites
- Harmonization of acoustic, turbulence, and power-curve procedures
- Demonstration of PV-VBT microgrids with synchronized logging instrumentation [107], [108], [110]

b) Midterm (3–6 years)
- Validation of hybrid passive-active resonance-tuning mechanisms
- Cost-optimized composite structures using modular manufacturing
- First large-scale rooftop and urban demonstration platforms [120], [121]

c) Long term (6–10 years)
- Full certification pathways aligned with IEC 61400-2 annexes
- Autonomous predictive maintenance enabled by AI and multi-sensor fusion
- Competitive LCOE for hybrid PV-VBT microgrids and decentralized smart-grid applications [115], [118], [119].

Through the combined development of durable structures, adaptive control systems, efficient hybrid PV-wind integration, and emerging certification frameworks, VBTs can progress from experimental prototypes to standardized, reliable, and environmentally responsible micro-wind generators capable of supporting next-generation distributed renewable energy systems.

8. Conclusion and Outlook

If these conditions are met, VBTs may evolve toward multi-kilowatt architectures offering competitive areal power density, silent operation, and natural interoperability with hybrid smart microgrids [10], [23], [49]. Progress in fluid-structure interaction modeling, composite materials, fatigue-resistant design, power electronics, and AI-driven optimization is expected to accelerate the emergence of next-generation VBT systems [10], [25], [26]. Reinforced by standardized validation pathways and solar-hybrid integration, vortex bladeless turbines hold strong potential as reliable, low-impact contributors to distributed renewable-energy ecosystems, complementing photovoltaic generation and strengthening the architecture of decentralized microgrids.

This review has consolidated the scientific and technological foundations of vortex bladeless turbines (VBTs), emphasizing the link between vortex-induced vibration (VIV) physics and their potential deployment in emerging renewable-energy architectures [24], [30], [31], [35], [96], [97], [102]. Their operation is fundamentally shaped by the lock-in phenomenon, during which the vortex-shedding frequency synchronizes with the natural frequency of the mast, enabling sustained oscillations and effective electromechanical transduction. Techniques based on stiffness and mass tuning-whether passive, semi-active, or hybrid-extend this synchronization window and mitigate the effects of turbulence, improving the predictability of the harvested power under transient atmospheric conditions [17], [27], [34], [35], [98], [100].

Materials science remains central to ensuring long-term structural reliability. High-modulus composites, sandwich configurations, and hybrid piezoelectric or electromagnetic transducers enhance stiffness-to-weight ratios, damping characteristics, and power density. Yet these gains require validation through multi-year fatigue campaigns, particularly to characterize adhesive-joint behavior, depolarization effects, and crack initiation under repeated VIV loading [21], [22], [54], [67], [97], [99], [103], [104]. At larger deployment scales, the compact wake generated by VBTs supports high areal power density and spatially efficient layouts, offering a viable alternative to conventional beam-swept turbines in constrained environments [14], [30], [31].

A key outcome of this review is the confirmed compatibility between VBTs and solar-dominated microgrids. Their rectified DC output integrates naturally with PV inverters and storage units, enabling hybrid PV-VBT systems where daytime photovoltaic production is complemented by evening or nocturnal wind generation [13], [23], [49], [107], [109]. This temporal synergy improves resilience and system availability while moderating storage requirements in regions characterized by strong solar irradiance and moderate nighttime winds, as observed in North Africa and the Moroccan Sahara [33], [83]. Silent operation, absence of rotating components, and minimal maintenance further position VBTs as suitable candidates for rooftops, coastal sites, and microgrid environments where acoustic and safety constraints are critical [13], [14], [23].

For the technology to reach full maturity, three structural pillars must be consolidated.

- **First**, standardized testing and certification-building on IEC 61400-2, are needed to harmonize procedures for power-curve characterization, turbulence classification, acoustic limits, mechanical qualification, and grid interfacing [14], [90].
- **Second,** long-term endurance datasets (≥ 5 years) remain essential to validate fatigue resistance, transducer longevity, and structural stability across diverse climatic conditions [22], [21], [54], [67].
- **Third,** transparent techno-economic assessments - including harmonized LCOE metrics, capacity-factor definitions, O&M schedules, and end-of-life considerations - are required to benchmark competitiveness relative to conventional micro-wind technologies [14], [90], [115], [116], [117], [118], [*119*].

If these conditions are met, VBTs may evolve toward multi-kilowatt architectures offering competitive areal power density, silent operation, and natural interoperability with hybrid smart microgrids [10], [23], [49]. Progress in fluid-structure interaction modeling, composite materials, fatigue-resistant design, power electronics, and AI-driven optimization is expected to accelerate the emergence of next-generation VBT systems [10], [25], [26], [101], [122], Reinforced by standardized validation pathways and solar-hybrid integration, vortex bladeless turbines hold strong potential as reliable, low-impact contributors to distributed renewable-energy ecosystems, complementing photovoltaic generation and strengthening the architecture of decentralized microgrids.

Acknowledgments

This research was conducted with the technical and academic support of the Faculty of Sciences of Ain Chock, Hassan II University of Casablanca, and the Renewable Energy and Sustainable Development Laboratory (LERDS). The authors also thank the Association ENERGIES for its involvement in renewable energy outreach and its assistance during site-level investigations related to microgrid integration and experimental validation of bladeless turbine concepts. The constructive discussions within the research team greatly contributed to improving the physical modeling, simulation, and interpretation of the results presented in this study.

Nomenclature

a) List of Acronyms

Acronym	Meaning
AC	Alternating Current
ACO	Ant Colony Optimization
AI	Artificial Intelligence
CFD	Computational Fluid Dynamics
CSM	Coupled Structural Model
DC	Direct Current
DC Bus	Direct Current Electrical Bus
DEM	Data-Enabled Modeling (if used in the article)
DOF	Degree of Freedom
EM	Electromagnetic
FFT	Fast Fourier Transform
FSI	Fluid–Structure Interaction
HAWT	Horizontal-Axis Wind Turbine
IEC	International Electrotechnical Commission
LCOE	Levelized Cost of Energy
PE	Piezoelectric
PRISMA	Preferred Reporting Items for Systematic Reviews and Meta-Analyses
PSO	Particle Swarm Optimization
PV	Photovoltaic
PV Curve	Power–Velocity Curve
RL	Reinforcement Learning
RMS	Root Mean Square
ROM	Reduced-Order Model
STOA	Solar–Thermal–Optical Alignment (if used in the article)
VAWT	Vertical-Axis Wind Turbine
VBT	Vortex Bladeless Turbine
VIV	Vortex-Induced Vibrations

b) Nomenclature – Physical Symbols

Symbol	Description	Unit
A	Oscillation amplitude	m
c	Damping coefficient	N·s/m
C_p	Power coefficient	–
D	Characteristic diameter of mast	m

E	Young's modulus (composite mast)	GPa
f	Vibration frequency	Hz
F_D	Drag force	N
FL	Lift force	N
f_s	Strouhal shedding frequency	Hz
$G(\theta,t)$	Solar irradiance (orientation, time)	W/m²
H	Mast height	m
k	Stiffness coefficient	N/m
m	Oscillating mass	kg
P	Instantaneous power generated	W
P_{avg}	Average power	W
P_{PV}	Photovoltaic output power	W
P_{VBT}	Turbine output power	W
Q	Quality factor	–
Re	Reynolds number	–
SOC	State of charge (battery)	%
S_t	Strouhal number	–
U	Free-stream wind velocity	m/s
U_c	Cut-in velocity	m/s
η	Conversion efficiency	–
ζ	Damping ratio	–
θ	Phase angle	rad
ρ	Air density	kg/m³
σ_f	Fatigue stress	Pa
ω	Forced vibration frequency	rad/s
ω_n	Natural angular frequency	rad/s

References

[1] Pourasl, H. H., Barenji, R. V., & Khojastehnezhad, V. M. (2023). Solar energy status in the world: A comprehensive review. *Energy Reports*, *10*, 3474–3493. https://doi.org/10.1016/j.egyr.2023.10.022

[2] Ahmed, S., Ali, A., Ansari, J. A., Qadir, S. A., & Kumar, L. (2025). A comprehensive review of solar photovoltaic systems: Scope, technologies, applications, progress, challenges, and recommendations. *IEEE Access*, *13*, 69723–69750. https://doi.org/10.1109/ACCESS.2025.3558539

[3] Hajou, A., & El Mghouchi, Y. (2025). Solar energy potential assessment in the MENA and Mediterranean regions. *Journal of King Saud University – Engineering Sciences*, 37, Article 42. https://doi.org/10.1007/s44444-025-00052-4

[4] Eze, V., Kiiza, R., Ukagwu, K. J., & Okafor, W. (2024). Factors influencing the efficiency of solar energy systems. *Journal of Engineering Technology and Applied Science*, *6*, 119–131. https://doi.org/10.36079/lamintang.jetas-0603.748

[5] Ayadi, O., Rinchi, B., Al-Dahidi, S., Abdalla, M. E. B., & Al-Mahmodi, M. (2024). Techno-economic assessment of bifacial PV systems under desert climatic conditions. *Sustainability*, *16*, 6982. https://doi.org/10.3390/su16166982

[6] Belmahdi, B., Louzazni, M., Akour, M., Cotfas, D. T., Cotfas, P. A., & El Bouardi, A. (2021). Long-term global solar radiation prediction in Morocco using FFNN-BP. *Frontiers in Energy Research*, 9, Article 733842. https://doi.org/10.3389/fenrg.2021.733842

[7] Rico-Riveros, L. F., Trujillo-Rodríguez, C. L., Díaz-Aldana, N. L., & Rus-Casas, C. (2025). Sustainable hybrid microgrid for rural electrification: Solar, biomass, and storage. *Applied Sciences*, 15, Article 10646. https://doi.org/10.3390/app151910646

[8] Ali, M. F., Sheikh, M. R. I., Ashikuzzaman, M., & Julhash, M. M. (2024). Sustainable solar–wind hybrid microgrid for rural electrification. In *Proceedings of the 27th International Conference on Computer and Information Technology (ICCIT)* (pp. 2032–2037). IEEE. https://doi.org/10.1109/ICCIT64611.2024.11021720

[9] Merino, C., & Castro, R. (2024). Optimization of a hybrid solar–wind microgrid for sustainable development: Case study in Antofagasta, Chile. *Sustainability*, 16, Article 3668. https://doi.org/10.3390/su16093668

[10] Manwell, J. F., McGowan, J. G., & Rogers, A. L. (2009). *Wind energy explained: Theory, design and application*. Hoboken, NJ: Wiley. https://doi.org/10.1002/9781119994367

[11] El Hadri, Y., Khokhlov, V., Slizhe, M., & Sernytska, K. (2019). Wind energy land distribution in Morocco (2021–2050) according to CORDEX-Africa RCM simulations. *Arabian Journal of Geosciences*, 12, Article 753. https://doi.org/10.1007/s12517-019-4950-7

[12] Yáñez Villarreal, D. J. (2018). *VIV resonant wind generators: Vortex Bladeless* (Technical brief). Vortex Bladeless S.L. https://vortexbladeless.com/wp-content/uploads/2018/10/VortexGreenPaper_en.pdf

[13] Nguyen, T. V., Tran, T. K., Dinh, H. H., & Ho, N. H. B. (2022). *Bladeless wind turbines* (Science-Policy Brief for the UN STI Forum). United Nations. https://sdgs.un.org/sites/default/files/2022-

05/2.4.9-17-Nguyen-Bladeless%20wind%20turbines.pdf

[14] Su, B., Guo, T., & Alam, M. M. (2025). A review of wind energy harvesting technology: Civil engineering resource, theory, optimization, and application. *Applied Energy*, 389, 125771. https://doi.org/10.1016/j.apenergy.2025.125771

[15] Islam, M., Ali, U., & Mone, S. (2024). Harnessing flow-induced vibrations for energy harvesting. *PLOS ONE*, 19, Article e0304489. https://doi.org/10.1371/journal.pone.0304489

[16] Cao, D., He, J., Zeng, H., Zhu, Y., Chan, S. Z., Williams, M. R., & Ghoshal, R. (2025). A review of oscillators in hydrokinetic energy harnessing through vortex-induced vibrations. *Fluids*, 10(4), Article 78. https://doi.org/10.3390/fluids10040078

[17] Breen, J., Mallik, W., & Adhikari, S. (2025). Performance analysis and geometric optimization of bladeless wind turbines using a wake oscillator model. *Renewable Energy*, 254, 123549. https://doi.org/10.1016/j.renene.2025.123549

[18] Peddigari, M., Kim, G.-Y., Park, C., Min, Y., Kim, J.-W., Ahn, C.-W., & Hwang, G. (2019). Fatigue behavior of piezoelectric macro-fiber composites for vibration energy harvesting. *Sensors*, 19, Article 2196. https://doi.org/10.3390/s19092196

[19] Mohamed, Z., Soliman, M., & Feteha, M. (2025). Optimal design of bladeless wind turbines using composite materials. *Scientific Reports*, 15, Article 1355. https://doi.org/10.1038/s41598-024-82385-9

[20] Han, D., Huang, S., Hui, P., & Yue, C. (2024). Development of a new type of vortex bladeless wind turbine for urban energy systems. *arXiv preprint*. https://doi.org/10.48550/arXiv.2410.13506

[21] Anusonti-Inthra, P., & Floros, M. (2008). Coupled CFD and particle vortex transport method: Wing performance and wake validations. In *38th AIAA Fluid Dynamics Conference and Exhibit*. https://doi.org/10.2514/6.2008-4177

[22] Sofamel S.A. (2023). *Vortex Bladeless reinvents wind energy* (White paper). https://sofamel.com/fr/b/informations/nouvelles/p/vortex-bladeless-reinventa-la-energia-eolica-49-2

[23] Bahadur, I. (2022). Dynamic modeling and investigation of a tunable vortex bladeless wind turbine. *Energies*, 15, Article 6773. https://doi.org/10.3390/en15186773

[24] Canilho, H., Fael, C., & Páscoa, J. (2020). A numerical study of vortex-induced vibrations on a circular cylinder under elastic support. *KnE Engineering*. https://doi.org/10.18502/keg.v5i5.6925

[25] Nejadali, J. (2024). Design improvement of small-scale VIV bladeless turbines. *Iranian Journal of Science and Technology, Transactions of Mechanical Engineering*, 48(4), 1839–1850. https://doi.org/10.1007/s40997-023-00739-6

[26] Yang, K., Kwak, G., Ch., K., & Huh, J. (2019). Wind farm layout optimization for wake effect uniformity. *Energy*, 183, 983–995. https://doi.org/10.1016/S0360-5442(19)31346-5

[27] Pranupa, S., Sriram, A., & Rao, S. N. (2023). Review of wind farm layout optimization techniques. *International Journal of Renewable Energy Research*, 13, 957–965. https://doi.org/10.20508/ijrer.v13i2.13935.g8768

[28] González-González, E., Yáñez, D. J., Del Pozo, S., & Lagüela, S. (2024). Optimizing bladeless wind turbines: Morphological analysis and lock-in range variations. *Applied Sciences*, 14, Article 2815. https://doi.org/10.3390/app14072815

[29] Kang, H., Kook, J., Lee, J., & Kim, Y.-K. (2024). A novel small-scale bladeless turbine using VIV and discrete resonance-shifting modules. *Applied Sciences*, 14, Article 8217. https://doi.org/10.3390/app14188217

[30] Van Dyke, M. (1982). *An album of fluid motion*. Stanford, CA: The Parabolic Press. https://courses.washington.edu/me431/handouts/Album-Fluid-Motion-Van-Dyke.pdf

[31] Ketata, A., Chelbi, L., Abid, H., & Driss, Z. (2025). Experimental investigation of the dynamic response of bladeless VIV turbines in a wind tunnel. *Engineering, Technology and Applied Science Research*, 15(5), 26612–26618. https://doi.org/10.48084/etasr.12314

[32] Jurasz, J., Bochenek, B., Wieczorek, J., Jaczewski, A., Kies, A., & Figurski, M. (2025). Energy potential and economic viability of small-scale wind turbines. *Energy*, 322, 135608. https://doi.org/10.1016/j.energy.2025.135608

[33] El Hafdaoui, H., Khallaayoun, A., & Al-Majeed, S. (2025). Renewable energies in Morocco: A comprehensive review. *Energy Conversion and Management X*, 26, 100967. https://doi.org/10.1016/j.ecmx.2025.100967

[34] Mendez, L., Narvarte, L., Marsinach, A. G., Izquierdo, P., Carrasco, L. M., & Eyras, R. (2003). Centralized stand-alone PV system in microgrid in Morocco. In *Proceedings of the 3rd World Conference on Photovoltaic Energy Conversion* (Vol. 3, pp. 2326–2328). IEEE. https://ieeexplore.ieee.org/document/1305054

[35] Luo, F., Gao, C., & Zhang, W. (2022). The key to suppress vortex-induced vibration: Stability of the structural mode. *Journal of Fluids and Structures*,

113, 103692. https://doi.org/10.1016/j.jfluidstructs.2022.103692
[36] Karthikeyan, S., & Nallayarasu, S. (2023). CFD simulation of VIV of an elastic cylinder in subcritical flow with two-way coupling. *Ocean Engineering*, 273, 113956. https://doi.org/10.1016/j.oceaneng.2023.113956
[37] Hamdan, H., Dol, S. S., Gomaa, A. H., Tahhan, A. B. A., Al Ramahi, A., Turkmani, H. F., & Ajaj, R. (2024). Experimental and numerical study of a novel vortex bladeless turbine with economic feasibility analysis. *Energies*, 17, Article 214. https://doi.org/10.3390/en17010214
[38] Francis, S., & Swain, A. (2024). Modelling and harnessing energy from flow-induced vibration: An explicit review. *Ocean Engineering*, 312, 119290. https://doi.org/10.1016/j.oceaneng.2024.119290
[39] Hajou, A., El Mghouchi, Y., & Chaoui, M. (2024). New solar–wind complementarity index: Application to Morocco. *Renewable Energy*, 227, 120490.
https://doi.org/10.1016/j.renene.2024.120490
[40] Meister, R., Yaïci, W., Moezzi, R., Gheibi, M., Hovi, K., & Annuk, A. (2025). Evaluating balancing properties of wind and solar PV production. *Energies*, 18, Article 1871. https://doi.org/10.3390/en18071871
[41] Mas'ud, A. A., Seidu, I., Salisu, S., Musa, U., AlGarni, H. Z., Bajaj, M., & Zaitsev, I. (2025). Wind energy assessment and hybrid microgrid optimization for Saudi Arabian regions. *Scientific Reports*, 15, Article 1376. https://doi.org/10.1038/s41598-025-85616-9
[42] Mishra, J., & Shankar, A. (2025). Optimizing wind–PV–battery microgrids for resilient residential communities. *Scientific Reports*, 15, Article 24339. https://doi.org/10.1038/s41598-025-06354-6
[43] Taha, H. M., & Mohammed, L. A. (2025). Hybrid photovoltaic–wind power systems for renewable microgrids: A review. *IOP Conference Series: Earth and Environmental Science*, 1507(1), Article 012005. https://doi.org/10.1088/1755-1315/1507/1/012005
[44] Hajou, A., El Mghouchi, Y., Yakoubi, H., Abdou, N., & Chaoui, M. (2021). Climate zoning based on solar radiation intensity in Morocco. *Energy Conversion and Management*, 247, 114770. https://doi.org/10.1016/j.enconman.2021.114770
[45] Merrouni, A. A., Elalaoui, F. E., Mezrhab, A., Mezrhab, A., & Ghennioui, A. (2018). Large scale PV sites selection by combining GIS and Analytical Hierarchy Process: Case study: Eastern Morocco. *Renewable Energy*, *119*, 863–873. https://doi.org/10.1016/j.renene.2017.10.044
[46] Wang, L., Kisi, O., Zounemat-Kermani, M., Salazar, G. A., Zhu, Z., & Gong, W. (2016). Solar radiation prediction using different techniques: Model evaluation and comparison. *Renewable and Sustainable Energy Reviews*, *61*, 384–397. https://doi.org/10.1016/j.rser.2016.04.024
[47] Amir, M., Singh, K., & Bashir, M. (2026). Optimal frequency control in renewable-dominated microgrids using a tilted controller optimized via salp swarm algorithm. *Energy Conversion and Management: X*, *29*, 101407. https://doi.org/10.1016/j.ecmx.2025.101407
[48] Belmahdi, B., Louzazni, M., Marzband, M., & El Bouardi, A. (2023). Hybrid meteorological model for global radiation forecasting: Morocco case. *Forecasting*, *5*, 172–195. https://doi.org/10.3390/forecast5010009
[49] Yang, H., Yin, Y., & Abu-Siada, A. (2025). A comprehensive review of solar panel performance degradation and adaptive mitigation strategies. *IET Control Theory & Applications*, 19, Article e70040. https://doi.org/10.1049/cth2.70040
[50] Rajendran, G., Raute, R., & Caruana, C. (2025). A comprehensive review of solar PV integration with smart grids: Challenges, standards, and grid codes. *Energies*, 18, Article 2221. https://doi.org/10.3390/en18092221
[51] Al-Rasheedi, M., & Al-Khayat, M. (2025). Assessing wind and solar energy complementarity using residual-load metrics. *Energy*, 335, 138107. https://doi.org/10.1016/j.energy.2025.138107
[52] Chizfahm, A., Azadi Yazdi, E., & Eghtesad, M. (2018). Dynamic modeling of vortex-induced vibration wind turbines. *Renewable Energy*, 121, 632–643.
https://doi.org/10.1016/j.renene.2018.01.03
[53] Prasad, A., & Kay, M. (2025). Mapping solar–wind complementarity with BARRA. *Energies*, 18, Article 5452. https://doi.org/10.3390/en18205452
[54] Barata, A. L., Kiwata, T., Ueno, T., Samhuddin, S., & Hasanudin, L. (2022). Experimental investigation of bladeless power generator from wind-induced vibration. *International Journal of Renewable Energy Development*, 11(3). https://doi.org/10.14710/ijred.2022.43888
[55] Boddapati, K., & Arrieta, A. F. (2024). Structural multistability for multi-speed wind energy harvesting from VIV. *Smart Materials and Structures*, 33, 05048. https://doi.org/10.1088/1361-665X/ad7d54
[56] Canziani, F., Vargas, R., & Gastelo-Roque, J. A. (2021). Hybrid photovoltaic–wind microgrid

with battery storage for rural electrification: Case study in Peru. *Frontiers in Energy Research*, 8, 528571. https://doi.org/10.3389/fenrg.2020.528571

[57] Dosa, A., Olanrewaju, O. A., & Mora-Camino, F. (2025). Hybrid renewable microgrids: Design parameters, optimization, and demand response. *Energies*, 18, Article 5154. https://doi.org/10.3390/en18195154

[58] Mendyl, A., Demir, V., Omar, N., Orhan, O., & Weidinger, T. (2024). Enhancing solar radiation forecasting in Moroccan climate zones using ML models with Sugeno aggregation. *Atmosphere*, 15, Article 103. https://doi.org/10.3390/atmos15010103

[59] Mundu, M. M., Sempewo, J. I., Nnamchi, S. N., Mahoro, G. B., & Uti, D. E. (2025). Integration of wind-flow effects into solar power generation models. *Scientific Reports*, 15, Article 8939. https://doi.org/10.1038/s41598-025-90680-2

[60] Anand, M., & Reghu, R. (2022). Design and optimization of a bladeless turbine. In *Proceedings of INDICON 2022*. https://doi.org/10.1109/INDICON56171.2022.10040205

[61] Dol, S. S., & Hamdan, H. (2024). Application of Vortex Bladeless turbines at offshore platforms for sustainable energy. In *ADIPEC 2024* (Paper D041S141R007). https://doi.org/10.2118/222566-MS

[62] Francis, S., Umesh, V., & Shivakumar, S. (2021). Design and analysis of vortex bladeless wind turbine. *Materials Today: Proceedings, 47*(16), 5584–5588. https://doi.org/10.1016/j.matpr.2021.03.469

[63] Yan, B., Ren, H., Li, D., Yuan, Y., Li, K., Yang, Q., & Deng, X. (2022). Numerical simulation for vortex-induced vibration of a high-rise building. *International Journal of Structural Stability and Dynamics, 22*. https://doi.org/10.1142/S0219455422400107

[64] Nnabuife, S. G., Quainoo, K. A., Hamzat, A. K., Darko, C. K., & Agyemang, C. K. (2024). Combining solar and wind with green hydrogen: Innovative strategies. *Applied Sciences, 14*, 9771. https://doi.org/10.3390/app14219771

[65] Breen, J., Mallik, W., & Adhikari, S. Performance analysis and geometric optimization of bladeless wind turbines using wake oscillator model. *Renewable Energy*, 254 (2025), 123549. https://doi.org/10.1016/j.renene.2025.123549

[66] Lafuente-Cacho, M., Izquierdo-Monge, O., Peña-Carro, P., Hernández-Jiménez, Á., Callejo, L. H., Palomares Losada, A. M., & Zorita Lamadrid, Á. L. (2025). State of the art of solar and wind forecasting methods for sustainable grid integration. *Current Sustainable/Renewable Energy Reports, 12*, 13. https://doi.org/10.1007/s40518-025-00262-z

[67] Ribeiro, L., Saavedra, O., de Matos, J., Lima, S., Bonan, G., & Martins, A. (2010). Design, control, and operation of a hybrid renewable system. *Eletrônica de Potência, 15*(4), 313–322. https://doi.org/10.18618/REP.2010.4.313322

[68] Huera-Huarte, F. J. (2026). Energy harvesting from vortex-induced vibrations using a pendulum. *Journal of Fluids and Structures, 140*, 104449. https://doi.org/10.1016/j.jfluidstructs.2025.104449

[69] Ali, M. F., Sheikh, M. R. I., Akter, R., Islam, K. M. N., & Ferdous, A. H. M. I. (2025). Grid-connected hybrid PV/wind/battery microgrids for rural education in Bangladesh. *Results in Engineering, 25*, 103774. https://doi.org/10.1016/j.rineng.2024.103774

[70] Roman, M., Sobh, R., Sedrak, M., & Ali, M. (2021). Power performance enhancement of VIV wind turbines using a semi-active control approach. *Energy Sources, Part A, 47*(2). https://doi.org/10.1080/15567036.2021.2006830

[71] Mihramane, R. L., Ech-Charqaouy, S. S., Saifaoui, D., Ech-Charqaouy, N., & Ech-Charqaouy, A. (2025). Management and optimization of a renewable-energy hybrid microgrid under voltage-stability constraints. *International Journal of Renewable Energy Research, 15*(2), 213–225. https://doi.org/10.20508/ijrer.v15i2.14781.g9042

[72] Ech-Charqaouy, S. S., Saifaoui, D., Benzohra, O., & Lebsir, A. (2020). Impact of integrating renewable energies into distribution networks on the voltage profile. *International Journal of Renewable Energy Research*, 10(1), 143–154. https://doi.org/10.20508/ijrer.v10i1.10204.g7848

[73] Pasetto, A., Tonan, M., Moro, F., & Doria, A. (2025). Design parameters affecting the performance of VIV harvesters. *Micromachines, 16*, 122. https://doi.org/10.3390/mi16020122

[74] Raafat, A., Kamra, M., & Al Nuaimi, S. (2025). Vortex-induced vibration of a deformable cylinder for wide lock-in range energy harvesting. *Engineering Applications of Computational Fluid Mechanics, 19*(1). https://doi.org/10.1080/19942060.2025.2514654

[75] Fershalov, A., Elvin, N., Orlandini, P., Avros, I., & Liu, Y. (2025). Harvesting sustainable energy through vortex-induced vibrations of finite-length cylinders. *Physics of Fluids, 37*(4), 04108. https://doi.org/10.1063/5.0260317

[76] Tenorio, G. L., Ortega, J., Ortíz, L., & Marín-Calvo, N. (2024). Stiffness impact on Vortex

Bladeless turbines. In *9th International Engineering, Sciences and Technology Conference* (pp. 210–215). https://doi.org/10.1109/IESTEC62784.2024.10820226

[77] Zhang, B., Li, B., Fu, S., Ding, W., & Mao, Z. (2022). Experimental investigation of high damping on VIV energy converters near the free surface. *Energy, 244*, 122677. https://doi.org/10.1016/j.energy.2021.122677

[78] Bahmani, M., & Akbari, H. (2010). Effects of mass and damping ratios on VIV of a circular cylinder. *Ocean Engineering, 37*, 511–519. https://doi.org/10.1016/j.oceaneng.2010.01.004

[79] Madi, L. S., Vernizzi, G. J., Defensor Filho, W. A., Kogishi, A. M., & Pesce, C. P. (2025). Experimental validation of a VIV-based energy harvester with orthotropic bending stiffness. In *OMAE2025 Conference Proceedings* (Paper V005T09A067). https://doi.org/10.1115/OMAE2025-157483

[80] Chhaparwal, G. K., & Dayal, R. (2023). Vortex-induced vibrations for energy harvesting: A review. In D. Sharma & S. Roy (Eds.), *Emerging trends in energy conversion and thermo-fluid systems* (pp. 275–284). Springer. https://doi.org/10.1007/978-981-19-3410-0_22

[81] Zhang, X., Chen, D., Luo, Y., Lin, Y., Liu, J., & Pan, G. Vortex-induced vibration characteristics of rigidly connected four-cylinder systems and nonlinear energy sinks for vibration suppression. Physics of Fluids, 36 (2024), 065120. https://doi.org/10.1063/5.0207583

[82] Cong, Y., Wei, D., Kang, H., Su, X., & Jiang, Y. Theoretical and CFD investigation on nonlinear dynamics of a cable under VIV with different aerodynamic shapes. Journal of Fluids and Structures, 125 (2024), 104061. https://doi.org/10.1016/j.jfluidstructs.2023.104061

[83] Pahlavanzadeh, M., Mohammadimehr, M., Irani-Rahaghi, M., & Emamat, S. Vibration response on the rod of a vortex bladeless generator with sandwich beam configurations. Mechanics Based Design of Structures and Machines, 53 (2024), 1–27. https://doi.org/10.1080/15397734.2024.2391920

[84] Fernandez-Aldama, R., Lopez-Garcia, O., Cuerva-Tejero, A., Gallego-Castillo, C., & Avila-Sanchez, S. Comparison of vortex-shedding models for wind turbine tower dynamics. AIP Conference Proceedings, 3030(1) (2024), 010007. https://doi.org/10.1063/5.0193302

[85] International Electrotechnical Commission. IEC 61400-2: Design requirements for small wind turbines. IEC, Geneva, Switzerland (2013). https://webstore.iec.ch/en/publication/5433

[86] Hafizh, M., Muthalif, A. G. A., Renno, J., Paurobally, M. R., Bahadur, I., Ouakad, H., & Ali, M. S. M. Vortex-induced vibration energy harvesting using magnetically coupled circular-array piezoelectric patches. Energy Conversion and Management, 276 (2023), 116559. https://doi.org/10.1016/j.enconman.2022.116559

[87] Zhang, G., Ma, M., & Lin, Y.-J. VIV-based passive flow sensor for fluidic flowmeters: Theoretical and experimental contributions. IEEE Transactions on Instrumentation and Measurement, 74 (2025), 1–9. https://doi.org/10.1109/TIM.2025.3562998

[88] Gharghani, F., Bijarchi, M. A., Mohammadi, O., & Shafii, M. Experimental investigation of a novel small-scale VIV-based energy-harvesting device. International Journal of Low-Carbon Technologies, 16 (2020). https://doi.org/10.1093/ijlct/ctaa060

[89] Marticorena, B., Bergametti, G., Gillette, D., & Belnap, J. Factors controlling threshold friction velocity in semiarid and arid areas. Journal of Geophysical Research: Atmospheres, 102 (1997), 23277–23288. https://doi.org/10.1029/97JD01303

[90] El-Shahat, A. Bladeless wind turbine as future wind energy technology. Natural Gas & Electricity, 33 (2016), 16–20.

[91] Marcollo, H., Behan, M., & Dillon-Gibbons, C. Universal screening criteria for VIV of free spans (V*). Journal of Marine Science and Engineering, 13 (2025), 1501. https://doi.org/10.3390/jmse13081501

[92] Bošnjaković, M. Analysis of CSP potential in a PV competitive landscape. Technologies, 13 (2025), 554. https://doi.org/10.3390/technologies13120554

[93] González, F. A., Posada, J., França, B. W., & Rosas-Caro, J. C. Inertia in converter-dominated microgrids: Control and estimation. Electricity, 6 (2025), 58. https://doi.org/10.3390/electricity6040058

[94] C. R., S., Mani, G., Alexander, S. A., Peter, G., Kumaresan, P., & Ganji, V. Expert system control in solar-PV-dominated microgrids: A critique. IET Renewable Power Generation, 19 (2023). https://doi.org/10.1049/rpg2.12875

[95] Fershalov, A., Albano, J., Orlandini, P., Elvin, N., & Liu, Y. Harvesting sustainable energy through vortex-induced cylinder vibrations. Proceedings of the ASME Fluids Engineering Conference (2024), Paper V001T03A004. https://doi.org/10.1115/FEDSM2024-124115

[96] Bakhtiar, S., Khan, F. U., Fu, H., Hajjaj, A. Z., & Theodossiades, S. Fluid-flow-based vibration energy harvesters: A critical review. Applied

Sciences, 14 (2024), 11452. https://doi.org/10.3390/app142311452
[97] Xu, W., Qin, W., & Gao, X. Experimental study on streamwise VIV of a flexible slender cylinder. Applied Sciences, 8 (2018), 311. https://doi.org/10.3390/app8020311
[98] Chen, J., Cai, H., Li, X., Li, X., & He, L. Numerical investigation on damping-ratio effects for flow-induced vibration of tandem cylinders. Physics of Fluids, 36 (2024), 077150. https://doi.org/10.1063/5.0213096
[99] Lo, J. C. C., Hourigan, K., Thompson, M. C., & Zhao, J. Effect of structural damping on flow-induced vibration of a thin elliptical cylinder. Journal of Fluid Mechanics, 974 (2023), A5. https://doi.org/10.1017/jfm.2023.776
[100] Alam, M. M. Effects of mass and damping on flow-induced vibration of a cylinder interacting with another wake at high reduced velocities. Energies, 14 (2021), 5148. https://doi.org/10.3390/en14165148
[101] Shahsavari, A., Afsharfard, A., & Kim, K. C. Enhancement of FIV-based energy harvesting in bladeless wind turbines through a downstream obstacle. Journal of Renewable and Sustainable Energy, 16 (2024), 053303. https://doi.org/10.1063/5.0222043
[102] Wen, Q., Schulze, R., Billep, D., Otto, T., & Gessner, T. Modeling and optimization of a VIV fluid kinetic energy harvester. Procedia Engineering, 87 (2014), 779–782. https://doi.org/10.1016/j.proeng.2014.11.656
[103] Patel, P., Agrawal, A., Sharma, A., & Bhardwaj, R. Experimental validation of VIV for circular and square cylinders with low and high mass damping. In Proceedings of the Fluid Mechanics and Fluid Power Conference (FMFP 2022). Springer (2022). https://doi.org/10.1007/978-981-99-5752-1_46
[104] Ren, H., Zhang, M., Cheng, J., Cao, P., Xu, Y., Fu, S., & Liu, C. Experimental investigation on VIV of a flexible pipe under higher modes in oscillatory flow. Journal of Marine Science and Engineering, 8 (2020), 408. https://doi.org/10.3390/jmse8060408
[105] Lee, Y. J., Qi, Y., Zhou, G., & Lua, K. B. VIV wind energy harvesting using a piezoelectric MEMS device in formation. Scientific Reports, 9 (2019), 20404. https://doi.org/10.1038/s41598-019-56786-0
[106] Wu, L., Weng, S., Zhu, H., Zhang, L., & Dai, H. Optimizing multi-frequency excitations for piezoelectric VIV energy harvesting. Smart Materials and Structures, 34(10) (2025), 05035. https://doi.org/10.1088/1361-665X/ae138e
[107] Mucomole, F. V., Silva, C. A. S., & Magaia, L. L. Parametric forecast of solar energy using machine learning techniques: Systematic review. Energies, 18 (2025), 1460. https://doi.org/10.3390/en18061460
[108] Srimanickam, B., Devi, V. V., Sarasu, P., et al. Performance evaluation of a hybrid solar collector with dryer: Experimental and ML-based study. Scientific Reports (2025). https://doi.org/10.1038/s41598-025-29714-8
[109] Alktranee, M., & Bencs, P. Overview of the hybrid solar system. Analecta Technica Szegedinensia, 14 (2020), 100–108. https://doi.org/10.14232/analecta.2020.1.100-108
[110] Jan-ngurn, C., & Bhumkittipich, K. Integration of solar and wind power with energy storage using discrete balancing. In Proceedings of the 9th International Electrical Engineering Congress (iEECON) (2021), 201–204. https://doi.org/10.1109/iEECON51072.2021.9440241
[111] Naeem, A., Ul Hassan, N., & Arshad, N. Design of solar–wind hybrid systems using complementarity. In Proceedings of the 4th International Conference on Green Energy and Applications (ICGEA) (2020), 100–105. https://doi.org/10.1109/ICGEA49367.2020.239713
[112] Zhang, W., Li, M., & Chen, Q. Optimizing standalone wind–solar–hydrogen systems: Hybrid renewables and electrolyzer coordination for green hydrogen. Processes, 13 (2025), 3801. https://doi.org/10.3390/pr13123801
[113] Gbadega, P. A., & Balogun, O. A. Modeling and control of grid-connected solar–wind hybrid microgrid using multi-input Ćuk converter. International Journal of Engineering Research in Africa, 58 (2022), 191–224. https://doi.org/10.4028/www.scientific.net/JERA.58.191
[114] Jiang, H., Yao, L., Qin, J., Bai, Y., Brandt, M., Lian, X., Davis, S. J., Zhao, W., Liu, T., & Zhou, C. Globally interconnected solar–wind system for future electricity demand. Nature Communications, 16 (2025), 4523. https://doi.org/10.1038/s41467-025-59879-9
[115] Salkuti, S. R. Techno-economic analysis of renewable energy, storage, and electric vehicles for sustainable development. Energies, 18 (2025), 238. https://doi.org/10.3390/en18020238
[116] Bilal, M., Ahmad, F., Mohammad, A., & Rizwan, M. Techno-economic evaluation and sensitivity analysis of renewable-energy-based EV

charging considering load-following strategy. Applied Energy, 377 (2025), 124557. https://doi.org/10.1016/j.apenergy.2024.124557

[117] Zakaria, A., & Singh, R. Techno-economic analysis for designing renewable energy systems in El-Fasher, Sudan. In Proceedings of the 15th International Conference on Power, Energy, and Electrical Engineering (CPEEE) (2025), 414–420. https://doi.org/10.1109/CPEEE64598.2025.10987487

[118] Samatar, A. M., Lekbir, A., Mekhilef, S., et al. Techno-economic and environmental analysis of a fully renewable hybrid energy system for sustainable infrastructure advancement. Scientific Reports, 15 (2025), 12140. https://doi.org/10.1038/s41598-025-96401-z

[119] Thango-Mabizela, B., & Obokoh, L. Techno-economic analysis of hybrid renewable energy systems for power interruptions: A systematic review. Engineering, 5 (2024), 2108–2156. https://doi.org/10.3390/eng5030112

[120] Bouafia, M., El Fathi, A., & El Akchioui, N. Techno-economic optimization of renewable-energy system sizing using metaheuristic and hybrid algorithms. Scientific African, 28 (2025), e02712. https://doi.org/10.1016/j.sciaf.2025.e02712

[121] Padmajaya, I., Aprillia, B. S., Raharjo, J., Adam, K. B., Oktavia, D. A., & Rahmat, B. Economic feasibility of a solar–wind hybrid power system in Telkom University. In Proceedings of the 19th International Multi-Conference on Systems, Signals & Devices (SSD) (2022), 964–968. https://doi.org/10.1109/SSD54932.2022.9955969

[122] Chen, J., Chen, M., & Liu, M. CFD simulation of vortex-induced motion of a caisson during installation. Journal of Physics: Conference Series, 2519 (2023), 012031. https://doi.org/10.1088/1742-6596/2519/1/012031